

## Prediction of shunting malfunction for track circuit based on combined analysis

ZHENG Yunshui, LI Yujie

(College of Automation & Electrical Engineering, Lanzhou Jiaotong University, Lanzhou 730070, China)

**Abstract:** Aiming at fault prediction for track circuit is restricted by data, the six-terminal network model is established based on the working principle and transmission line theory of ZPW-2000A track circuit to simulate and analyze three kinds of shunting malfunction signals. A combined analysis method combining variational mode decomposition and convolutional neural network is proposed. The energy spectrum feature is extracted from the original signal by variational mode decomposition, and the deep feature is extracted by convolution neural network. Then, the sensitive feature for fault prediction is obtained by weighted fusion of the two. The simulation experiments indicate that the proposed method can predict the shunting malfunction accurately and effectively, which can achieve a prediction accuracy of 99.87% and provide a new idea for the prediction of the shunting malfunction for track circuit.

**Key words:** track circuit; shunting malfunction; variational mode decomposition; deep learning; feature fusion

### 0 Introduction

As important basic equipment of railway signals, track circuit plays the roles of train occupied inspection and transmission of train information, and its working state is directly related to the transportation efficiency and operation safety. Track circuit will be short-circuited by train wheelsets when occupied, so the current flowing through the receiver is less than its working threshold, so the track relay falls indicating that the section is occupied by the train. However, track circuit cannot be shorted well in shunting malfunction, so the current keeps the track relay on. Therefore, it cannot give the indication of the section being occupied. The phenomenon of shunting malfunction may threaten the safety of operation, such as route release in advance, switch in transition halfway and so on. According to statistics, there are more than 36 000 shunting malfunction sections in the whole road in China. Among all kinds of train operation accidents, more than 30% are caused by shunting malfunction<sup>[1]</sup>.

At present, the researches on shunting malfunction mainly focus on the formation mechanism. With the development of computer

technology, many intelligent methods have been applied to the fault prediction for track circuit. The research on the fault prediction usually requires a lot of data, and the existing studies have shown that the data simulated by track circuit model can replace the field data<sup>[2-6]</sup>. Wang<sup>[2]</sup> adopted the fuzzy entropy theory and the principle of asymmetric closeness to establish an early warning system of shunting malfunction, which made the early warning more accurate. Feng<sup>[3]</sup> proposed a shunt resistance estimation method based on the received voltage amplitude of locomotive signal at the transmitter, which provided a new method for the prediction of shunting malfunction. Zhang<sup>[4]</sup> extracted the feature based on wavelet analysis, and the prediction model of PSO-SVM was used to realize the prediction of shunting malfunction. However, the prediction model takes a longer time due to the large amount of calculation when the experimental samples are too large.

A six-terminal network model is established by analyzing the working principle and transmission characteristics of track circuit to simulate the shunting current signal caused by shunting malfunction. In order to improve the accuracy and

**Received date:** 2022-11-29

**Foundation items:** Regional Science Fund Program of National Natural Science Foundation of China (No. 61763023)

**Corresponding author:** LI Yujie (347598816@qq.com)

stability of prediction, the variational mode decomposition applied in signal processing is combined with the deep learning of artificial intelligence algorithm. The feasibility of this method is verified by the training set data and the test set data. And compared with others, the combined analysis method improves the accuracy and stability of prediction.

## 1 Six-terminal network model of shunting state for track circuit

### 1.1 Six-terminal network model

In the actual train operation, the frequency shift signal generated by the transmitter has leakage to the ground in the transmission process of the rail lines, so the rail lines can be considered as a three-

conductor transmission line<sup>[7]</sup>. The six-terminal network model is established for the parts greatly affected by the ground, e. g., the main track circuit and syntonics sections, and the four-terminal network model is established for the parts with better ground insulation protection in the transmission channel and the receiving channel. By simulating the process of the train body entering track circuit, it is found that the shunt resistances of the wheelset are approximately the same when the train wheelset is considered as single wheelset and multiple wheelsets respectively entering the same track circuit section<sup>[8-9]</sup>. Therefore, to simplify the model, single wheelset is used to equivalent the situation that track circuit has been occupied. The shunting state of ZPW-2000A track circuit is modelled, as shown in Fig. 1.

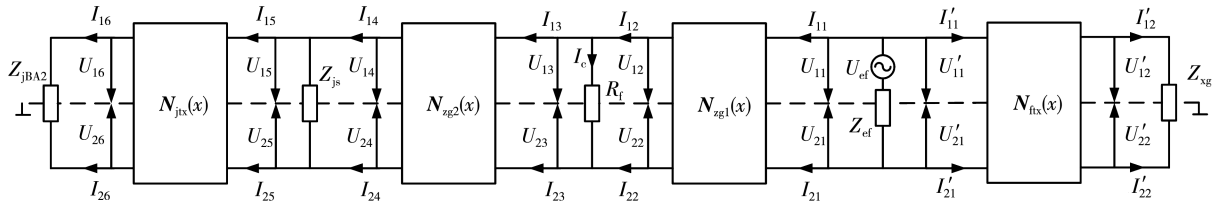


Fig. 1 Six-terminal network model of shunting state for track circuit

In Fig. 1,  $Z_{jBA2}$  is the equivalent impedance of the sytonic unit BA1;  $Z_{js}$  is the apparent impedance between the receiver sytonic unit BA1 and the receiver;  $R_f$  is the shunt resistance of the first wheelset of the train;  $Z_{zg}$  is the apparent impedance from the transmitter sytonic unit BA2 to the receiver of small track. According to Thevenin's theorem, the circuit between the transmitter sytonic unit BA1 and the transmitter can be equivalent to a series connection of a voltage source  $U_{ef}$  and an impedance  $Z_{ef}$ .

According to the transmission line theory, the transmission matrix equation of the six-terminal network model can be obtained as

$$\begin{bmatrix} U_{11} \\ U_{21} \\ I_{11} \\ I_{21} \end{bmatrix} = \mathbf{N}_{zg1}(x) \mathbf{N}_R(R_f) \mathbf{N}_{zg2}(x) \mathbf{N}_{js}(Z_{js}) \mathbf{N}_{jtx}(x) \begin{bmatrix} U_{16} \\ U_{26} \\ I_{16} \\ I_{26} \end{bmatrix}, \quad (1)$$

where  $U_{11}$  and  $U_{21}$  are the ground voltages of rails at both ends of  $U_{ef}$  and  $Z_{ef}$ , respectively;  $I_{11}$  and  $I_{21}$  are the current of rail at both ends of  $U_{ef}$  and  $Z_{ef}$ , respectively;  $U_{16}$  and  $U_{26}$  are the ground voltage of rails at both ends of  $Z_{jBA2}$ ;  $I_{16}$  and  $I_{26}$  are the current of rails at both ends of  $Z_{jBA2}$ ;  $\mathbf{N}_{zg_l}(x)$  ( $l = 1, 2$ )

represents the transmission characteristic matrix of the main track circuit with length  $x$ ;  $\mathbf{N}_R$  ( $R_f$ ) represents the transmission characteristic matrix of  $R_f$ ;  $\mathbf{N}_{js}$  ( $Z_{js}$ ) represents the transmission characteristic matrix of  $Z_{js}$ ;  $\mathbf{N}_{jtx}(x)$  represents the transmission characteristic matrix from  $Z_{js}$  to  $Z_{jBA2}$ .

For the transmitter sytonic section, Kirchhoff's law shows that

$$\begin{bmatrix} U'_{11} \\ U'_{22} \\ I'_{11} \\ I'_{22} \end{bmatrix} = \mathbf{N}_{ftx}(x) \begin{bmatrix} U'_{12} \\ U'_{22} \\ I'_{12} \\ I'_{22} \end{bmatrix}, \quad (2)$$

$$\begin{bmatrix} 1 & -1 & -Z_{jBA2}/2 & Z_{jBA2}/2 \\ 0 & 0 & 1 & 1 \end{bmatrix} \begin{bmatrix} U'_{12} \\ U'_{22} \\ I'_{12} \\ I'_{22} \end{bmatrix} = \mathbf{0}_{2 \times 1}, \quad (3)$$

where  $U'_{11}$  and  $U'_{21}$  are the ground voltages of rails at both ends of  $U_{ef}$  and  $Z_{ef}$ , respectively;  $I'_{11}$  and  $I'_{21}$  are the current of rail at both ends of  $U_{ef}$  and  $Z_{ef}$ , respectively;  $U'_{12}$  and  $U'_{22}$  are the ground voltage of rails at both ends of  $Z_{jBA2}$ ;  $I'_{12}$  and  $I'_{22}$  are the current of rails at both ends of  $Z_{jBA2}$ ;  $\mathbf{N}_{ftx}(x)$  represents the transmission characteristic matrix from  $U_{ef}$  to  $Z_{jBA2}$ .

For the transmitter sytonic unit, Kirchhoff's law

shows that

$$\begin{bmatrix} 1 & -1 & -Z_{jBA2}/2 & Z_{jBA2}/2 \\ 0 & 0 & 1 & 1 \end{bmatrix} \begin{bmatrix} U_{16} \\ U_{26} \\ I_{16} \\ I_{26} \end{bmatrix} = \mathbf{0}_{2 \times 1}. \quad (4)$$

The voltage and current on both sides of the transmitter satisfy the relationship of

$$\begin{bmatrix} 1 & 0 & 0 & 0 \\ 0 & 1 & 0 & 0 \\ 0 & 0 & 1 & 1 \\ 1 & -1 & Z_{ef}/2 & -Z_{ef}/2 \end{bmatrix} \begin{bmatrix} U_{11} \\ U_{21} \\ I_{11} \\ I_{21} \end{bmatrix} + \begin{bmatrix} -1 & 0 & 0 & 0 \\ 0 & -1 & 0 & 0 \\ 0 & 0 & 1 & 1 \\ 0 & 0 & Z_{ef}/2 & -Z_{ef}/2 \end{bmatrix} \begin{bmatrix} U'_{11} \\ U'_{21} \\ I'_{11} \\ I'_{21} \end{bmatrix} = \begin{bmatrix} 0 \\ 0 \\ 0 \\ U_{ef} \end{bmatrix}. \quad (5)$$

The transmission equation between the transmitter and the shunt resistance can be expressed as

$$\begin{bmatrix} U_{11} \\ U_{21} \\ I_{11} \\ I_{21} \end{bmatrix} = \mathbf{N}_{zg1}(x) \begin{bmatrix} U_{12} \\ U_{22} \\ I_{12} \\ I_{22} \end{bmatrix}, \quad (6)$$

where  $\mathbf{N}_{zg1}(x)$  represents the transmission characteristic matrix from  $U_{ef}$  to  $R_f$ .

$U_{11}$  and  $U_{22}$  can be obtained from simultaneous Eq. (1) to Eq. (6), so the shunting current  $I_c$  is

$$I_c = (U_{12} - U_{22})/R_f. \quad (7)$$

$I_c$  can reflect the shunting condition of rail lines, so it plays an important role in the prediction of shunting malfunction. The shunting current signal is electromagnetically induced with the receiving coil of the locomotive signal, which is converted into the locomotive induced voltage signal to generate the train control information. There is only difference in amplitude coefficient between shunting current signal and locomotive induced voltage signal, so the detection of locomotive induced voltage signal is transformed into shunting current detection.

### 1.2 Influence of shunting malfunction

The model is simulated based on the line data of a certain electricity section. The length of the main track circuit is 1 176 m and the carrier signal is 1 700 Hz. Fig.2 shows the envelope curve of shunting current obtained by simulation, which is compared with the actual induced voltage envelope curve after normalization to verify the correctness of the six-terminal network model. The leakage to the

ground is considered by the six-terminal network model of track circuit established, so the obtained envelope curve of shunting current is more consistent with the actual data, which improves the accuracy of equivalent model. There are many reasons for shunting malfunction. It is thought that the shunt resistance increases, which causes the track circuit not to short well.

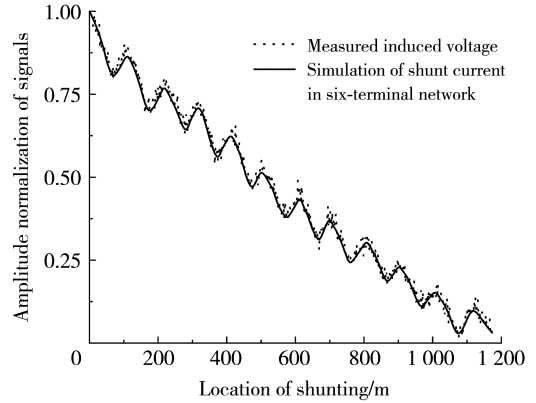


Fig. 2 Three signal amplitude normalization comparison

This paper mainly studies the instantaneous shunting malfunction or local shunting malfunction caused by the train passing through the neutral zone, braking sand or the wet section. Fig.3 shows the shunting malfunction of track circuit at 300 m—470 m. The curve of solid line represents the normal shunting, and the other three curves represent the situations that shunting malfunction are gradually serious.

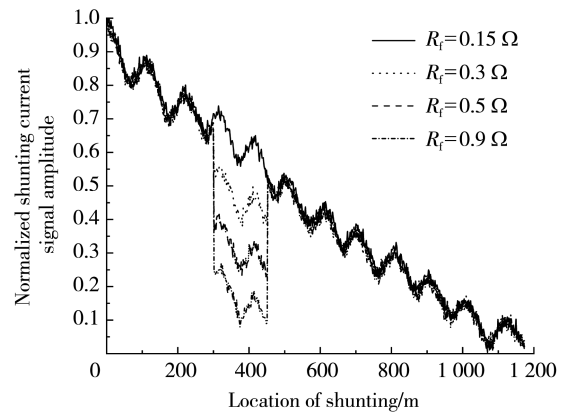


Fig. 3 Part of shunting malfunction of track circuit

It can be seen from Fig.3 that due to rail impedance, ballast resistance and other reasons, the signal is attenuated in the transmission process, so the amplitude envelope curve of shunting current shows attenuation trend. Due to compensation capacitance, the transmission channel tends to be resistive, and the attenuation of signal is slowed down, ensuring the transmission distance. If there is

a bad shunting between 370 m—400 m, the signal amplitude of the fault part is obviously lower than the normal signal amplitude. And with the increase of shunt resistance, the signal amplitude is lower, which indicates that the impact of shunting malfunction is more and more serious. However, the overall change trend of amplitude envelope curve of current is consistent with that of track circuit in normal condition.

## 2 Prediction of shunting malfunction of track circuit based on combined analysis

### 2.1 Combined analysis method

When the train moves into a certain section, the shunting current signal will be generated. Considering that the envelope signal of track circuit is non-linear and non-stationary, a combination of variational mode decomposition (VMD) and deep learning composed of cascade block convolutional neural network (CB-CNN) is proposed to predict the shunting malfunction for track circuit, as shown in Fig. 4.

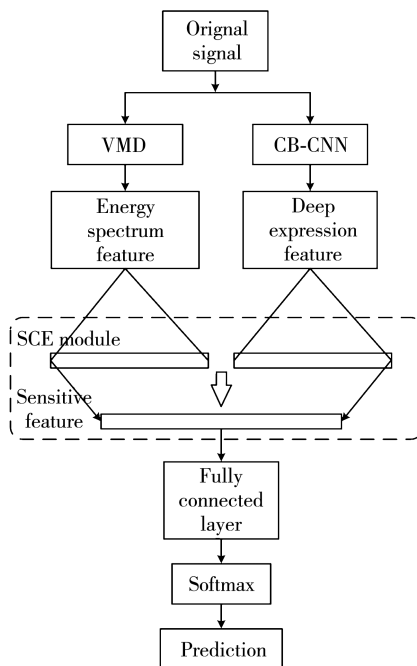


Fig. 4 Framework of combined analysis method

One branch is composed of VMD which is mainly used to decompose the original signal and extract the energy spectrum feature. The other is CB-CNN, which extracts the features through a series of operations such as convolution, pooling and so on by constructing filters with different features of the

input data. Then the SCE fusion module fuses the features extracted from the two branches to get the sensitive feature  $p$ . Finally, the normal signal and fault signal are classified by the back-end classifier to predict whether the track circuit has bad shunting.

The reason is that the two branches have complementary information. The left can reflect the frequency domain characteristics of signal, and the right can extract the abstract feature of the original signal by the multi-layer mapping of CB-CNN. The feature extracted by deep learning do not have clear physical meaning, and it is difficult to be analyzed. Whereas the feature extracted by signal processing has clear physical meaning. However the extraction of feature quantity is artificially selected, and the selection of different feature quantity will also affect the accuracy of prediction. In order to learn from each other, the two features are fused.

### 2.2 VMD

Non-recursive VMD is used to decompose the original signal into  $K$  eigenmode functions  $u_k(t)$ . The  $u_k(t)$  can be regarded as a frequency and amplitude modulation signal, so the original signal can be expressed as

$$f(t) = \sum_k u_k(t) = \sum_k A_k(t) \cos(\varphi_k(t)), \quad (8)$$

where  $A_k(t)$  and  $\varphi_k(t)$  are the instantaneous amplitude and phase of  $u_k(t)$ , respectively. Therefore, the VMD algorithm can be regarded as the original signal decomposed into  $K$  mode functions  $u_k(t)$ , and each component is iterated synchronously to minimize the sum of the estimated bandwidth of each component. The VMD algorithm consists of the 3 parts.

#### 1) Construction of variational problem

① The single side spectrum of  $u_k(t)$  is obtained by Hilbert transform for each  $u_k(t)$ , and the estimated center frequency  $\omega_k$  is mixed with each component to modulate each component to the baseband in frequency shift.

$$\left[ \left( \delta(t) + \frac{j}{\pi t} \right) * u_k(t) \right] e^{-j\omega_k t}, \quad (9)$$

where  $\delta(t)$  is the impulse function;  $*$  is a convolution operator.

② By calculating the square estimation bandwidth of L2 norm of each component, the constrained variational model is obtained.

$$\begin{cases} \min_{\{u_k\}, \{\omega_k\}} \left\{ \sum_k \left\| \partial t \left[ \left( \sigma(t) + \frac{j}{\pi t} \right) * u_k(t) \right] e^{-j\omega_k t} \right\|_2^2 \right\}, \\ \text{s. t. } \sum_k u_k(t) = f(t), \end{cases} \quad (10)$$

where  $\partial t$  is the gradient operation;  $\{u_k(t)\} = \{u_1(t), u_2(t), \dots, u_K(t)\}$  is the component;  $\{\omega_k\} = \{\omega_1, \omega_2, \dots, \omega_K\}$  is the central frequency;  $\| \cdot \|_2$  indicates L2-norms.

## 2) Solution of variational problem

By introducing the quadratic penalty factor  $\alpha$  and Lagrange multiplier  $\lambda(t)$ , the constrained variational problem of Eq. (10) can be transformed into unconstrained variational problem, shown as

$$\begin{aligned} L(\{u_k(t)\}, \{\omega_k\}, \lambda) = & \alpha \sum_k \left\| \partial t \left[ \left( \sigma(t) + \frac{j}{\pi t} \right) * u_k(t) \right] e^{-j\omega_k t} \right\|_2^2 + \\ & \left\| f(t) - \sum_k u_k(t) \right\|_2^2 + \left\langle \lambda(t), f(t) - \sum_k u_k(t) \right\rangle. \end{aligned} \quad (11)$$

$$m = \left[ \frac{E(u_1)}{\sum_{i=1}^k E(u_i)}, \frac{E(u_2)}{\sum_{i=1}^k E(u_i)}, \dots, \frac{E(u_k)}{\sum_{i=1}^k E(u_i)} \right] = [m_1, m_2, \dots, m_k]_{1 \times k}. \quad (14)$$

## 2.3 CB-CNN

The structure of CB-CNN is shown in Fig. 5. The original signal is convoluted through the convolution

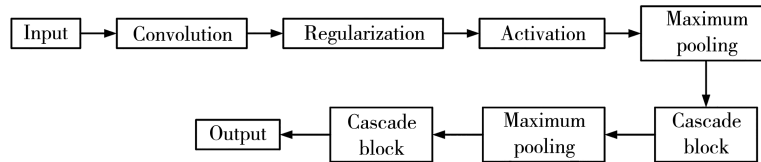


Fig. 5 Structure of CB-CNN

The cascade block has eight layers of operation, including three layers of convolution calculation, two layers of activation, one layer of upsampling, one layer of concatenate calculation and one layer of batch normalization. The detailed structure is shown in Fig. 6.

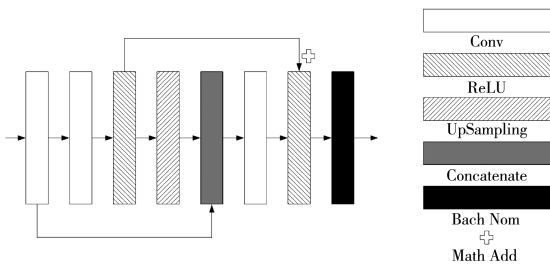


Fig. 6 Structure of cascade block

The three parameters  $u_k(t)$ ,  $\omega_k$  and  $\lambda(t)$  are updated by alternating direction multiplier method. When the condition of Eq. (12) is satisfied, the final solution of Eq. (11) can be obtained.

$$\frac{\sum_k (\|\hat{u}_k^{n+1}(\omega) - \hat{u}_k^n(\omega)\|_2^2)}{\hat{u}_k^n(\omega)} < \epsilon, \quad (12)$$

where  $\hat{u}_k^n(\omega)$  is the Fourier transform of  $u_k^n(t)$ , and the convergence error  $\epsilon > 0$ .

## 3) Extraction of feature

The signal decomposed by VMD can reflect the distribution characteristics in different frequency bands<sup>[10]</sup>, whereas the energy of fault signal in different frequency bands fluctuates greatly, so the energy spectrum feature of signal is used as the input of fault prediction. The energy value of each frequency band can be expressed as

$$E(u_i) = (u_i)^2, \quad (13)$$

where  $u_i$  represents the  $i$ -th component.

Therefore, the energy spectrum feature of the signal can be expressed as

layer, then through the regularization layer, activation layer and maximum pooling layer, and finally into the subsequent cascade block.

Since the non-stationary signal has a strong time correlation, this characteristic will gradually weaken as the depth of the cascade deepens. There are two bridging branches in the cascade block to preserve the temporal correlation of shallow features.

## 2.4 SCE module

The SCE module consists of four steps: squeeze, connect, excitation and reweight.

1) Squeeze. The feature matrix  $\mathbf{X} =$

$$\begin{bmatrix} x_{11} & \cdots & x_{1b} \\ \vdots & \vdots & \vdots \\ x_{a1} & \cdots & x_{ab} \end{bmatrix}_{a \times b}$$

extracted by CB-CNN is squeezed

by the global average pooling method to obtain

feature  $\mathbf{n}$ .

$$n_j = F_{sq}(\mathbf{X}) = \frac{1}{L} \sum_{i=1}^L x_{ij}, j = 1, 2, \dots, b, \quad (15)$$

$$\mathbf{n} = (n_1, n_2, \dots, n_b). \quad (16)$$

2) Connect. The squeezed feature  $\mathbf{n}$  is connected with the feature  $\mathbf{m}$  extracted by VMD to obtain the fusion feature  $\mathbf{q}$ .

$$\mathbf{q} = F_{co}(\mathbf{m}, \mathbf{n}) = (m_1, \dots, m_k, n_1, \dots, n_b, ) = (q_1, \dots, q_c), \quad (17)$$

and  $c = k + b$ .

3) Excitation. The weight  $\omega$  of feature  $\mathbf{q}$  is estimated by feature dimension reduction.

$$\omega = F_{ex}(\mathbf{q}, \mathbf{W}) = \sigma(g(\mathbf{q}, \mathbf{W})) = \sigma(\mathbf{W}_2 \delta(\mathbf{W}_1 \mathbf{q})), \quad (18)$$

where  $\mathbf{W}_1$  and  $\mathbf{W}_2$  are the mapping matrices obtained by learning;  $\sigma$  and  $\delta$  are the mapping functions.

4) Reweight. The feature  $\mathbf{q}$  is weighted to obtain the sensitive feature  $\mathbf{p}$  for prediction.

$$\mathbf{p} = F_{scale}(\mathbf{q}, \omega) = \omega \mathbf{q}. \quad (19)$$

### 3 Simulation and discussion

#### 3.1 Data source

In order to verify the feasibility and effectiveness of the proposed method in shunting malfunction prediction, the model established in 1.1 is adopted to simulate the shunting current under normal conditions and faults, and White Gaussian Noise is introduced to replace the environmental disturbance of the train. The four kinds of signals in Fig. 3 are simulated by setting different line parameters of track circuit, each type of signal has 2 500 sets, with a total of 10 000 sets of data. Among them, 7 000 sets are training set samples, and 3 000 sets are test set samples.

#### 3.2 Selection of parameters

##### 1) Selection of mode decomposition number $K$

Since the classification accuracy of the prediction model will be affected by the number of mode decomposition in VMD algorithm, the appropriate number of  $K$  is selected first. As shown in Fig. 7, the classification accuracy curve is obtained by using different mode decomposition numbers and training times on the training set. When the decomposition number  $K=4$ , the classification accuracy is relatively stable compared with other decomposition numbers.

The performance of each mode decomposition number in the training set and test set is shown in Table 1.

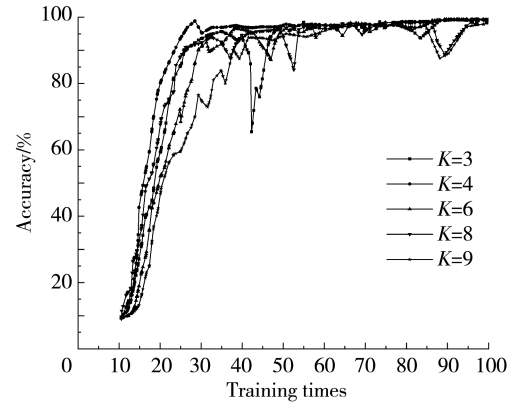


Fig. 7 Influence of different  $K$  on prediction model

Table 1 Classification accuracy of different  $K$

$K$	Training set accuracy/%	Test set accuracy/%
3	99.55	97.00
4	100.00	99.85
6	99.80	98.75
8	99.65	98.55
9	100.00	99.20

When the decomposition numbers are 3, 4, 6, 8 and 9, respectively, the classification accuracy of the prediction model in the training set is not different. However, when the decomposition number  $K=4$ , the prediction model shows better performance in both the training set and the test set, and has good generalization ability.

Therefore, the mode decomposition number  $K$  of the signal is selected as 4.

##### 2) Selection of convolution kernel for each module

The parameters selection of CB-CNN, SCE fusion module and classifier are shown in Table 2.

Table 2 Selection of parameters for each module

Module	Layer	Convolution kernel
CB-CNN	Convolution	64
	First cascade block	[32, 64]
	Second cascade block	[128, 256]
SCE	First fully connected	17
	Second fully connected	272
Classifier	First fully connected	100
	Second fully connected	4

#### 3.3 Simulation

##### 1) Signal decomposition

Fig. 8 shows the decomposition and comparison diagram of VMD for normal shunting ( $R_f=0.15 \Omega$ ) and fault ( $R_f=0.5 \Omega$ ).

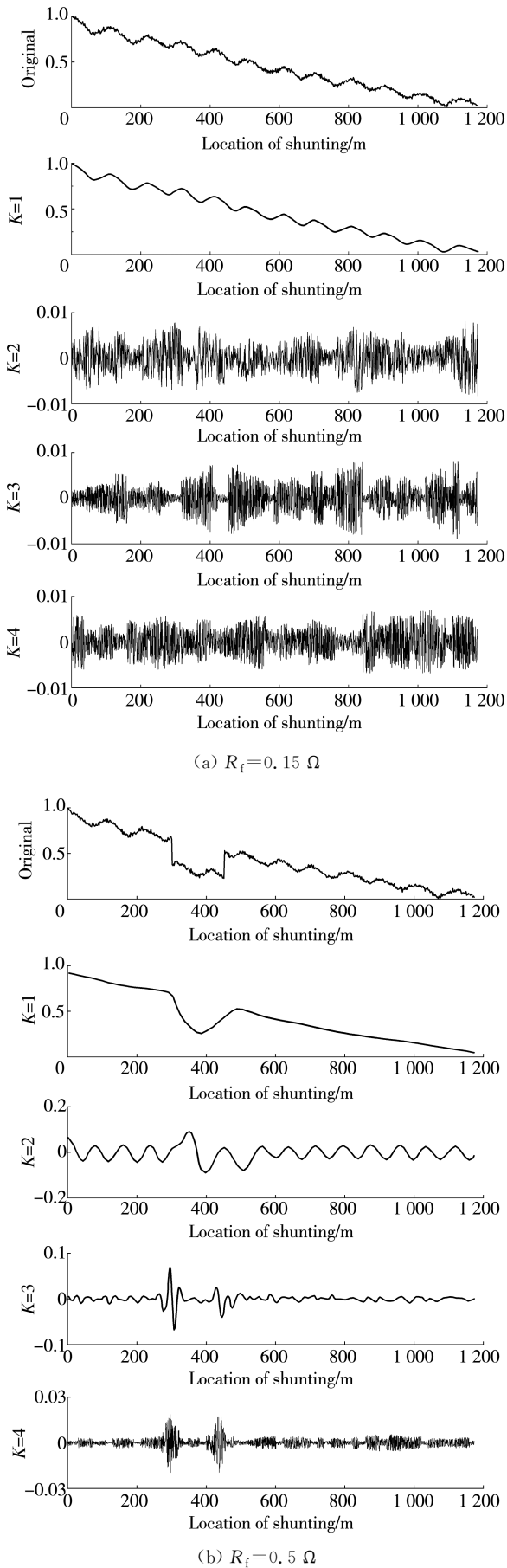


Fig. 8 VMD comparison diagram

When the track circuit is normal, the decomposed signals show regular fluctuations without abrupt signals. Whereas the track circuit has shunting malfunction, the fluctuation of some sections with bad shunting is significantly greater than that caused by noise. In addition, VMD can remove the attenuation trend of normal signal and smooth the signal to notice the fluctuation of the fault. Thus, VMD algorithm is effective for predicting shunting malfunction.

2) Network training

Fig. 9 shows the relationship between the number of iterations and the prediction accuracy. The network learning rate is set as 0.01, and the parameter fine-tuning is  $0.005^{[11]}$ .

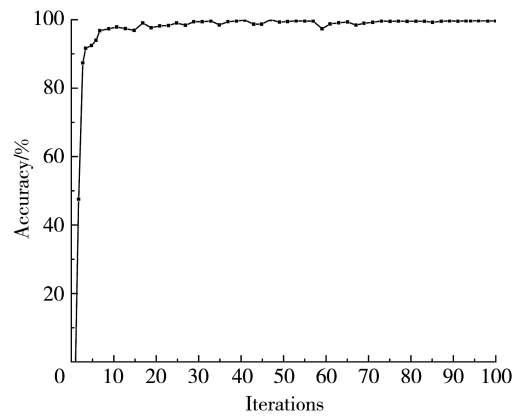


Fig. 9 Relationship between iterations and accuracy

After several iterations, the highest prediction accuracy reaches 100% and tends to be stable after the eighth iteration, indicating that the combined analysis method of VMD and CB-CNN can effectively predict the phenomenon of shunting malfunction for track circuit.

3.4 Discussion

In order to verify the superiority of the algorithm, the models of Refs. [4] and [14] are used to classify the data to predict the fault, and the average classification accuracy is shown in Table 3.

Table 3 Comparison results of combined method with other methods

Method	Accuracy/%
GWO-SVM	94.82
PSO-SVM	99.5
Combined analysis	99.87

It can be found that the combined analysis method is superior to other methods in classification accuracy, and its classification accuracy can reach more than 99.8%. Fig.10 shows the prediction result of shunting malfunction using the combined

analysis method.

The classification label of normal shunting is 1, and the other classification labels are bad shunting. The simulation experiments show that there are 2 groups, 1 group and 1 group of samples misclassified respectively when the classification label are 2, 3 and 4 in 3 000 test set samples, and the classification accuracy is 99.87%.

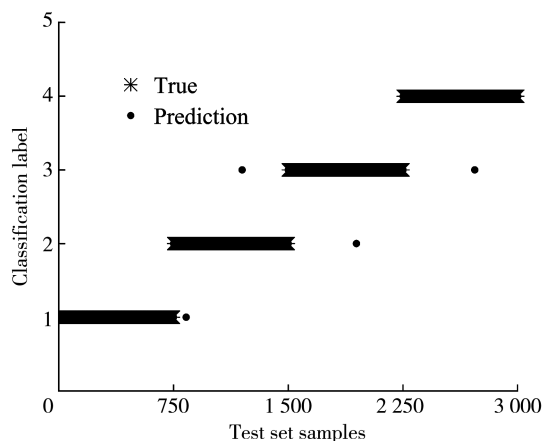


Fig. 10 Prediction results of shunting malfunction

## 4 Conclusions

In view of the shunting malfunction of track circuit, variational mode decomposition is combined with convolution neural network. The normal shunting current signal and fault signal are classified to achieve the effective prediction of shunting malfunction. By establishing the equivalent model of track circuit to simulate fault data. The energy spectrum feature is extracted by the variational mode decomposition algorithm, and the deep expression feature is extracted by deep learning. They are fused to obtain sensitive feature, which can achieve the effective prediction of bad shunting.

A new idea is proposed for the prediction of similar non-linear and non-stationary signals, and the parameters optimization method of VMD is also the focus of future research.

## References

- [1] HU Y S. Improvement plan of track circuit bad shunting. *Railway Signaling and Communication*, 2008(5): 24-26.
- [2] WANG R F, XI X N. On the safety warning to be made based on the fuzzy entropy and asymmetric proximity. *Journal of Safety and Environment*, 2017, 17(3): 829-834.
- [3] FENG D, ZHAO L H. Online estimation method of shunt resistance based on cab-signal remote monitoring system. *Journal of the China Railway Society*, 2017, 39(4): 62-67.
- [4] ZHANG M Q, ZHAO H B, SUN S P. Prediction of shunt malfunction of track circuit based on PSO-SVM. *Journal of the China Railway Society*, 2015, 37(10): 68-74.
- [5] XU K, ZHAO L H. A rapid diagnosis method for multiple compensation capacitor faults of jointless track circuits. *Journal of the China Railway Society*, 2018, 40(2): 67-72.
- [6] ZHANG Y P, QI H, ZHAO B. Research on method for detection of shunt state of track circuits. *Journal of the China Railway Society*, 2017, 39(1): 70-75.
- [7] FENG D, ZHAO L H. Modeling of JTC shunt states based on train structure and running scenarios. *Journal of Beijing Jiaotong University*, 2019, 43(2): 41-47+57.
- [8] NAGASE K, NOMURA T, HIRAMA J. Influence of contact condition between rails and wheels upon track circuit shunting (1st report quantitative evaluation of factors that cause inadequate track circuit shunting). *Transactions of the Japan Society of Mechanical Engineers, Part C*, 1997, 63(616): 4187-4194.
- [9] HIRAMA J, WAKABAYASHI Y, KITAGAWA T, et al. Influence of contact condition between rails and wheels upon track circuit shunting (4th report, result of continuously measured shunting resistance of the running wheelsets). *Transactions of the Japan Society of Mechanical Engineers, Part C*, 2005, 71(4): 1263-1268.
- [10] DING C J, FENG Y B, WANG M N. Rolling bearing fault diagnosis using variational mode decomposition and deep convolutional neural network. *Journal of Vibration and Shock*, 2021, 40(2): 287-296.
- [11] CHEN Z, HU Y Q, TIAN S Q, et al. Non-stationary signal combined analysis based fault diagnosis method. *Journal on Communications*, 2020, 41(5): 187-195.
- [12] SHAO H D, JIANG H K, ZHANG H Z, et al. Rolling bearing fault feature learning using improved convolutional deep belief network with compressed sensing. *Mechanical Systems and Signal Processing*, 2018, 100: 743-765.
- [13] HUANG B. Research on fault optimal combination prediction model of ZPW-2000A track circuit based on improved metabolic GM(1,1) and SVM. *Journal of Railway Science and Engineering*, 2019, 16(11): 2852-2858.
- [14] SU L N. Research on fault diagnosis of shunt malfunction for ZPW-2000A track circuit based on improved VMD and feature selection. Chengdu: Southwest Jiaotong University, 2019.
- [15] KI B L, SEJUNE C, CHANG O K. A convolutional neural network for fault classification and diagnosis in semiconductor manufacturing processes. *IEEE Transactions on Semiconductor Manufacturing*, 2017, 30(2): 135-142.
- [16] CHEN Z Q, DENG S C, CHEN X D, et al. Deep neural networks-based rolling bearing fault diagnosis. *Microelectronics Reliability*, 2017, 75: 327-333.



[17] JIANG G Q, HE H B, YAN J, et al. Multiscale convolutional neural networks for fault diagnosis of wind tur-

bine gearbox. IEEE Transactions on Industrial Electronics, 2019, 66(4): 3196-3207.

## 基于组合分析法的轨道电路分路不良预测

郑云水, 李钰婕

(兰州交通大学 自动化与电气工程学院, 甘肃 兰州 730070)

**摘要:** 针对轨道电路故障预测研究受数据制约的现象, 本文基于 ZPW-2000A 型轨道电路的工作原理和传输线理论, 建立了轨道电路六端网模型, 来仿真模拟 3 类分路不良故障信号, 并对其进行分析。同时, 提出变分模态分解和卷积神经网络结合的组合分析法, 对原始信号进行变分模态分解提取能量谱特征, 再与卷积神经网络提取的深度表达特征进行加权融合, 得到敏感特征用于故障预测。轨道电路分路不良预测的实验结果表明: 组合分析法能够准确有效预测分路不良故障, 预测的准确率达到 99.87%, 为轨道电路分路不良的预测提供了新的思路。

**关键词:** 轨道电路; 分路不良; 变分模态分解; 深度学习; 特征融合

**引用格式:** ZHENG Yunshui, LI Yujie. Prediction of shunting malfunction for track circuit based on combined analysis. Journal of Measurement Science and Instrumentation, 2023, 14(2): 233-241. DOI: 10.3969/j.issn.1674-8042.2023.02.013